AJNR

Radiologic-pathologic correlation. Bilateral retinoblastoma with coexistent pinealoblastoma (trilateral retinoblastoma).

J M Provenzale, A L Weber, G K Klintworth and R E McLendon

AJNR Am J Neuroradiol 1995, 16 (1) 157-165
http://www.ajnr.org/content/16/1/157.citation

Radiologic-Pathologic Correlation

Bilateral Retinoblastoma with Coexistent Pinealoblastoma (Trilateral Retinoblastoma)

James M. Provenzale, Alfred L. Weber, Gordon K. Klintworth, and Roger E. McLendon

From the Departments of Radiology (J.M.P.), Pathology (G.K.K., R.E.M.), and Ophthalmology (G.K.K.), Duke University Medical Center, Durham, NC, and the Department of Radiology (A.L.W.), Massachusetts Eye and Ear Infirmary, Boston, Mass

History

Clinical

Complete retinal detachment in the right eye and a large white, elevated tumor within the left retina were diagnosed in a 2-day-old girl. The patient's father had a history of bilateral retinoblastoma. Computed tomography (CT) of the orbits and brain was performed.

Headache, nausea, unsteady gait, and visual field defects developed when the patient was 2 years of age. Magnetic resonance (MR) imaging of the brain was performed.

Imaging

A noncontrast CT examination performed at age 18 days demonstrated bilateral intraocular masses (Fig 1A). A large mass lesion with predominantly high attenuation characteristics, consistent with calcification, was found in the right eye, filling most of the posterior globe. In the left eye, a smaller intraocular mass containing a few small punctate calcifications was seen. There was no evidence of extension into either orbit. CT findings of the brain were normal. On the basis of the patient's young age, the bilateral location, and the presence of calcification within the masses, bilateral retinoblastoma was diagnosed. Cerebrospinal fluid examination was negative for the presence of tumor cells. The right eye was enucleated at age 3 weeks. Radiation therapy was administered to the left eye, with tumor regression noted over the next few months.

MR imaging at age 2 years demonstrated a large, inhomogeneously enhancing mass lesion involving the pineal gland (Figs 1B–D). The mass had a large central region that was isointense with cerebrospinal fluid, consistent with necrosis (Fig 1B). Large portions of the mass were relatively isointense with gray matter on T2-weighted images (Fig 1D). At surgery a few days later, a pineal tumor with poorly defined margins was found, and most of the tumor was resected. Cytologic examination of the cerebrospinal fluid disclosed malignant cells. Systemic chemotherapy was initiated.

Pathology

The right eye contained a retinoblastoma that filled the entire contents of the globe posterior to the lens (Fig 1E). Extensive necrosis, characterized by a white, chalky fluid that oozed from the bisectioned specimen, was present. Microscopically, the tumor was confined to the globe and featured a monomorphous proliferation of cells with high nu-

Address reprint requests to James Provenzale, MD, Department of Radiology, Box 3808, Duke University Medical Center, Durham, NC 27710.

Index terms: Retina, neoplasms; Pineal gland, neoplasms; Children, neoplasms; Radiologic-pathologic correlations

AJNR 16:157–165, Jan 1995 0195-6108/95/1601–0157

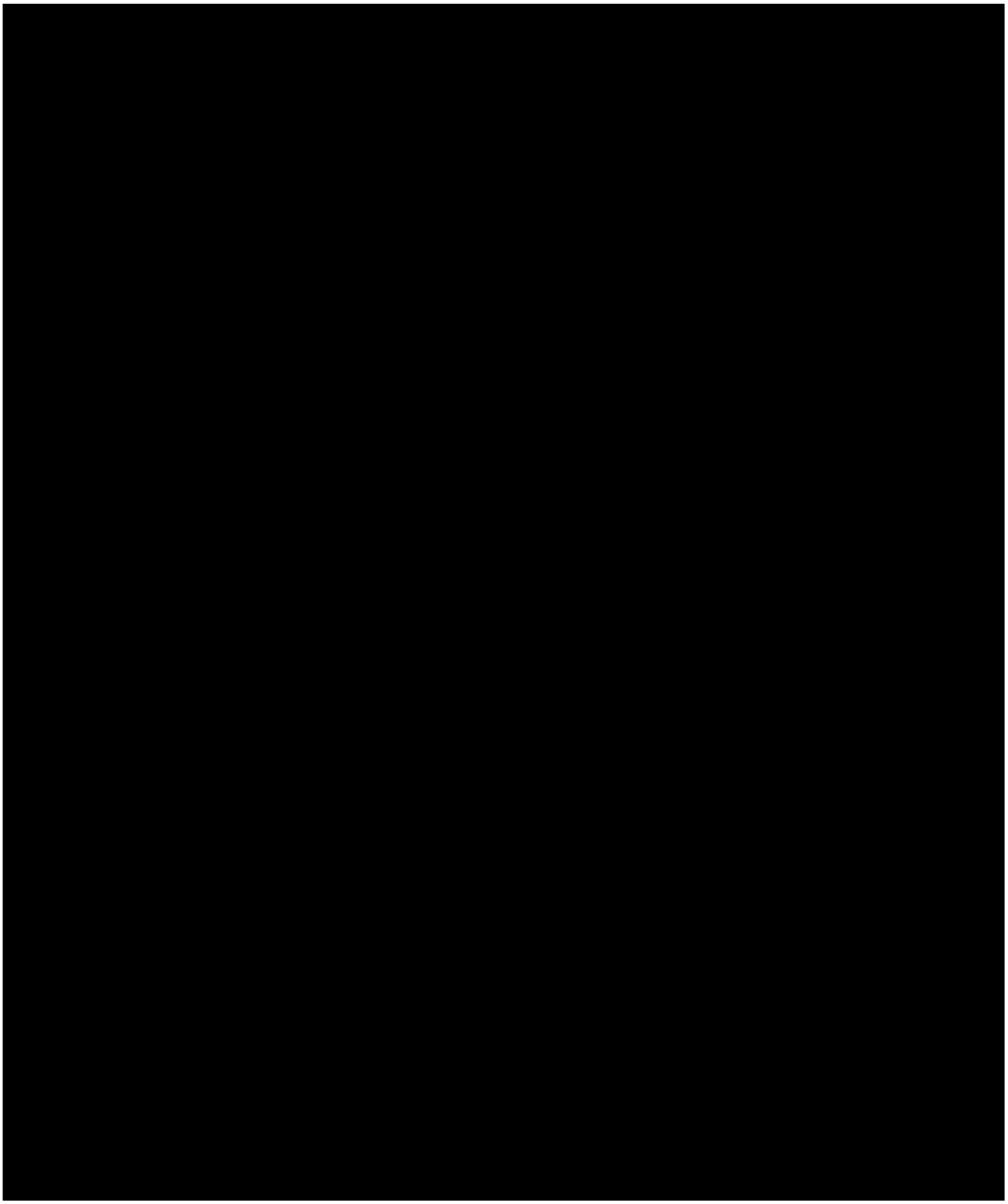

Fig 1. *A*, Noncontrast CT examination at age 18 days demonstrates bilateral intraocular masses. The mass in the right eye (*curved arrow*) has high attenuation characteristics, caused by diffuse calcification. The mass in the left eye is smaller and contains a few punctate calcifications (*arrows*).

B, Contrast-enhanced T1-weighted (500/11/2 [repetition time/echo time/excitations]) sagittal MR examination performed at 2 years of age. An inhomogeneous enhancing pineal mass is seen, causing obstructive hydrocephalus because of compression of the cerebral aqueduct (*arrow*). An irregularly marginated cystic component is present (*curved arrow*), consistent with a large

clear to cytoplasmic ratios, interspersed by cords of necrotic debris (Fig 1F). The bands of tumor cells were largely centered about blood vessels and were bounded by streaks of mineralized necrotic cellular debris. Flexner-Wintersteiner rosettes were widespread throughout the specimen (Fig 1G).

The pineal tumor was predominantly composed of small tumor cells with large nuclear-to-cytoplasmic ratios (Fig 1H). In particular, this finding was noted in the portions of the tumor that were isointense with gray matter on T2-weighted images. Abundant necrosis was present throughout the specimen, which caused it to break into many small fragments during processing for light microscopic examination. Perivascular rosettes were readily apparent, although no true neuronal rosettes were found.

Diagnosis

Bilateral retinoblastoma with coexistent pinealoblastoma ("trilateral retinoblastoma" syndrome).

Discussion

Incidence and Age

Retinoblastoma is the most common malignant intraocular neoplasm of childhood (1). The incidence of this tumor is between 1 in 15 000 and 1 in 30 000 live births (1–3), with approximately 200 new cases in the United States each year (4). The tumor occurs in both eyes in 25% to 40% of cases (1, 5). The average age at time of diagnosis in the United States is 13 months (6), but earlier in patients with family history of retinoblastoma because of anticipatory screening (7). The tumor is usually diagnosed during infancy, with the vast majority of cases diagnosed before the age of 2 years (6) and only about 8% of cases seen after the age of 5 years (8).

The term *trilateral retinoblastoma* has been used to refer to the presence of bilateral retinoblastomas with an associated primary intracranial neoplasm of primitive type (usually in the pineal region but occasionally in the suprasellar or parasellar region) (9, 10). Such a coexistent intracranial neoplasm is found in about 3% of patients with bilateral retinoblastoma (11). The intracranial tumor is considered a lesion distinct from the intraocular neoplasms, not a metastasis (9, 12). There is usually a latent period of a few years between diagnosis of the intraocular tumor and a coexistent intracranial lesion (13). Compared with spontaneous retinoblastomas, the ocular tumors in patients with trilateral retinoblastoma present at an earlier age (mean, 7.2 months) (12, 13). A positive family history of retinoblastoma is present in about 65% of cases (13).

Calcification is seen in approximately 95% of retinoblastomas examined histologically (14), a fact reflected in the high incidence of calcification detected by CT (3, 15–17). One prominent exception is diffuse infiltrat-

Fig 1, *Cont'd.*
region of necrosis.

C, Contrast-enhanced T1-weighted (500/11/2) axial image. There is asymmetric expansion of the tumor to the right. A portion of the nonenhancing necrotic region (*arrow*) is demonstrated.

D, T2-weighted (2900/80/1) axial image demonstrates that the mass is inhomogeneous, with much of the tumor being relatively isointense with gray matter (*arrowheads*). Note the transependymal resorption of cerebrospinal fluid (*curved arrow*) adjacent to the dilated lateral ventricles due to obstructive hydrocephalus.

E, Macroscopic appearance of the right eye after exenteration 1 week after the CT examination shown in A. An inhomogeneous white mass, representing an exophytic and endophytic retinoblastoma, fills almost the entire vitreous. On sectioning, the tumor, which was extensively necrotic, oozed a chalky white fluid. The tissue had a gritty texture because of widespread calcification, corresponding to the high attenuation appearance of the mass on noncontrast CT.

F, The tumor features a sea of small basophilic cells, interspersed by cords of calcified necrotic cellular debris (*arrowheads*). Numerous retinoblastomatous rosettes (*arrows*) are demonstrated (hemotoxylin and eosin; ×200).

G, The retinoblastomatous rosettes (*arrow*) featured well-defined central lumina with wispy eosinophilic material surrounded by a palisading rim of tumor cells. Numerous mitotic figures (*arrowheads*) were found throughout the tumor (hemotoxylin and eosin; ×400).

H, A specimen from the pineal neoplasm demonstrates a profusion of small tumor cells with high nuclear-to-cytoplasmic ratios. Large regions of cell death (one of which is outlined by arrowheads) were found, corresponding to the cystic regions demonstrated on MR imaging (hemotoxylin and eosin; ×300).

ing retinoblastoma, which may fail to calcify even when there is extensive involvement of the globe (18). This rare subtype of retinoblastoma, which accounts for 1% of cases, does not produce a discrete tumor mass, but a thick layer of tumor cells spread uniformly along the retina (19). This form of the tumor presents at a later age (approximately 6 years old), is much more frequently unilateral, and has a slower growth and more favorable prognosis than typical retinoblastoma (19).

Macroscopic Pathology

Retinoblastoma appears macroscopically as a single or multiple small white nodules within the retina. The tumor may grow endophytically toward the center of the globe and spread into the vitreous, or, alternatively, the tumor may grow exophytically behind the retina and result in retinal detachment (20). However, neither pattern has any prognostic significance. In contrast, presentation of tumor in the anterior chamber is a sign of a poor prognosis.

Microscopic Pathology

Histologically, the ocular tumor exhibited a monomorphous mass of small tumor cells with a high nuclear-to-cytoplasmic ratio imparting a blue tinctorial quality on histologic sections stained with hematoxylin and eosin. This sea of small blue cells is interrupted only by occasional strands of fibrous ensheathed blood vessels and the sometimes common, doughnutlike structures formed by the tumor cells arranged as spokes about a central lumen, the so-called Flexner-Wintersteiner, or true, retinoblastomatous rosettes (Fig 1G). A second specialized structure found within retinoblastomas is the fleurette, a structure that has been likened to a bouquet of flowers, with a cluster of long cytoplasmic processes simulating stalks, abutting a group of upward facing nuclei. A minority of retinoblastomas may also contain Homer Wright rosettes, similar to the true retinoblastomatous rosette although lacking a lumen. Larger tumors are frequently necrotic, with viable tumor cells crowding heavily about blood vessels amid puddles of eosinophilic cellular debris (Fig 1F). Calcification of the necrotic debris is commonly found (20, 21).

The blastomatous neoplasm that arises in the pineal gland, the final piece to this deadly troika, is histologically similar in appearance to the retinoblastoma (21). Hematoxylin and eosin-stained sections reveal a similarly undifferentiated small blue tumor cell forming occasional Homer-Wright rosettes and perivascular pseudorosettes. This similarity reflects the common phylogenetic origin of the retina and pineal gland as light-sensing organs. Immunohistochemical location of the rhodopsin-related S-antigen (arrestin) in the tumor cells lends visual support to the argument (22).

Genetics: Molecular Pathology of the Rb1 Gene

Having observed that familial retinoblastomas were often bilateral, in sharp contrast to the unilateral neoplasms of sporadic forms, Knudson proposed that retinoblastoma oncogenesis required at least two separate mutational events, or "hits," on the target cell genome (23). For the familial form of this neoplasm, he proposed that the first hit was inherited as a germline mutation present in all cells, with the second hit occurring as an acquired event. For the spontaneous form of the disease, he suggested that both hits were acquired phenomena on the same cell, and thus, less statistically likely to occur bilaterally (23). These hits have been found to take the form of a mutational deactivation of both alleles of a gene, which has become known as Rb1. As predicted for the familial form of retinoblastoma, the first hit is an inherited deletion of one allele in every cell with the second allele becoming inactivated by either a complete or partial deletion (24) or a mutational event (25) resulting in an inactive gene product. Furthermore, as predicted, the spontaneous form of retinoblastoma has two separately acquired somatic mutations in the retinal cells.

The molecular biological features of the Rb1 gene recently have been reviewed (26). Briefly, the Rb1 gene, located on chromosome 13 at locus q14, is encoded by 27 exons over 200 Kb of DNA. The 4.7 kb mRNA produced from the gene codes for an approx-

imately 110-kDa nuclear phosphoprotein product. Although its complete function is yet to be worked out, the gene is thought of as a tumor suppressor because of the ability of its gene product, the Rb1 protein, to suppress DNA replication. It is clear, however, that Rb1 deletion alone is not sufficient to induce malignant transformation in the retina. First, all retinoblastomas have chromosomal changes in addition to a homozygous loss of the gene (27, 28). Second, retinomas, or small benign retinal tumors, have been found in patients with germline deletions of Rb1 (29). These retinomas may progress to malignancy (27, 30), suggesting that additional genetic factors are involved in the transformation process (31). Finally, although the initial Rb1 mutation is present in all cells, the secondary tumors, which are most commonly osteosarcomas and soft-tissue sarcomas, arise within the irradiation fields, supporting the notion that irradiation-induced chromosomal damage is additionally needed for malignant transformation in these tumors (32). It is difficult to understand why Rb1 is so sharply focused on retinal neoplasia. One proposal is that retinal cells are uniquely dependent on Rb1 for critical control of cell cycle functions, functions that other cells apparently have "back-up" mechanisms of controlling.

Diagnosis

Clinical Features and Differential Diagnosis

Leukocoria (a white pupillary reflex) and strabismus are the most common clinical findings of retinoblastoma (33). Other much less common presenting features include a painful red eye, decreased vision, and orbital inflammation simulating orbital cellulitis (7, 8). When the ocular media are clear, a fundus tumor can be seen on ophthalmoscopy. The ocular media may be opaque, however, precluding ophthalmoscopic visualization (33). The major considerations in the clinical differential diagnosis when leukocoria or an ophthalmologically apparent fundus mass is present include neoplasms (primarily retinoblastoma, but also retinal astrocytoma), developmental abnormalities (eg, persistent hyperplastic primary vitreous and Coats disease), acquired retinal lesions (eg, retinopathy of prematurity and chronic retinal detachment), and infection (primarily endophthalmitis secondary to *Toxocara canis*) (34). Persistent hyperplastic primary vitreous is a congenital malformation in which abnormal regression and hyperplasia of the primary vitreous results in formation of a retrolental fibrovascular connective tissue mass (35). Coats disease is a congenital retinal telangiectasia characterized by fusiform dilatation of retinal vessels associated with a subretinal lipid-rich exudate, which often results in retinal detachment in the late stages of the process (36). The end result is a chronically detached retina with a prominent subretinal exudate that contains a considerable number of cholesterol crystals (37). The disease is usually seen in boys after the age of 4 years and, therefore, later than the vast majority of retinoblastomas (37). Ocular toxocariasis is a granulomatous response to a *Toxocara canis* larva, which results in a protein-rich subretinal inflammatory exudate. It is usually seen in older children (average age, 6 years), again later than the typical age of diagnosis of retinoblastoma (38). The diagnosis can be confirmed by means of an enzyme-linked immunosorbent assay for *Toxocara canis* (39). Whereas persistent hyperplastic primary vitreous is occasionally bilateral, Coats disease and ocular toxocariasis are almost always unilateral (37, 38).

Patterns of Metastasis

Invasion of the optic nerve by retinoblastoma, with subsequent dissemination to the subarachnoid space and central nervous system, is one of the principal means of extension of the tumor (40). Invasion of the ocular venous system can result in hematogenous dissemination and systemic metastases (41). The choroid, which is often infiltrated by tumor cells, serves as a site from which retinoblastoma can extend through the sclera and into the orbit (40). CT evidence of central nervous system metastases is seen in about 50% of retinoblastoma cases and may be seen up to a few years after tumor excision (42, 43). Almost all patients dying of retinoblastoma have metastases to the skull or brain, with extra–central nervous system metastases present in more than half of these

Differential diagnosis of some lesions causing leukocoria

	Typical Age	Laterality	Size of Globe	CT	MR	Ultrasound
Retinoblastoma	Usually <2 y	Unilateral or bilateral	Normal	Intraocular, usually calcified, mass	T1-weighted: Iso- or slightly hyperintense to vitreous; hypointense to vitreous on T2 weighted images	Highly echogenic mass, occasional distal shadowing
Persistent hyperplastic primary vitreous	Birth	Usually unilateral	Often small	Increased vitreal density; soft tissue along Cloquet's canal; occasional dependent layering of high-attenuation fluid in subretinal space	Hyperintense vitreous on both T1- and T2-weighted images. Occasional fluid-fluid level	Intravitreal band extending from posterior lens to optic disk
Coats disease	3–5 y	Usually unilateral	Normal	Diffuse increased density of globe and retinal detachment	Hyperintense subretinal effusion on T1- and T2-weighted images	Early: Multiple shallow retinal detachments Late: Diffuse retinal detachment
Toxocara endophthal-mitis	5–10 y	Unilateral	Normal	Noncalcified intraocular mass; irregularity and thickening of uveoscleral coat	Subretinal effusion, which is hyperintense on T1- and T2-weighted images	Elevated mass; vitreal membranes; retinal folds or detachment
Retinopathy of prematurity (advanced)	Birth	Bilateral	Often small	Microphthalmia; retinal detachments; shallow anterior chambers; Increased density of globes	Hyperintense subretinal effusion on T2-weighted images	"Looplike" appearance of peripheral retinal detachment

patients (41). There is an extremely high rate of subarachnoid spread of tumor in trilateral retinoblastoma, with spinal spread of tumor seen in almost all cases (13).

CT

CT is the mainstay of the radiologic diagnosis of retinoblastoma, primarily because of its sensitivity to calcification, an important feature distinguishing retinoblastoma from other entities with which it may be confused clinically (3, 15–17). Retinoblastoma is seen on CT as an intraocular mass lesion, which is calcified in about 95% of cases, located posterior to the lens (33). There is usually mild or moderate enhancement of the tumor after contrast administration (33, 37), which helps to separate tumor from accompanying subretinal effusion (38). The diagnosis is considered highly likely when intraocular calcifications are seen in a child younger than 3 years of age (15, 44), because none of the entities that simulate retinoblastoma tend to calcify in children of this age (see Table). Thus the presence of calcification within an intraocular mass in the 18-day-old child presented here significantly increased the likelihood of the diagnosis of retinoblastoma, as did the presence of a calcified mass in the other eye, because bilateral abnormalities are seen on CT in between 25% and 40% of cases.

Retinoblastoma calcifications may be single or multiple and vary in size from punctate to large, flocculent foci (15, 38). Large tumors have been reported to usually contain an inhomogeneous pattern of calcifications and small lesions a more homogeneous pattern (15, 17). In unusual cases, retinoblastoma is demonstrated solely as calcifications without an associated mass lesion or as an uncalcified mass (15, 33). As noted earlier, diffuse infiltrating retinoblastoma may not be demonstrated on CT as either calcified or a mass lesion. After the age of 3 years, the presence of calcification is less specific because some of the entities that simulate retinoblastoma (eg, retinal astrocytoma, toxocariasis, advanced Coats disease with retinal necrosis, and, rarely, advanced retinopathy of prematurity) can also be calcified (8, 38). However, all of these entities should be distinguishable from retinoblastoma by other radiologic findings and clinical features.

CT is an important tool in distinguishing retinoblastoma from lesions that simulate it. The CT findings in persistent hyperplastic primary vitreous can include (*a*) a diffuse high-attenuation appearance of the vitreous; (*b*) a triangular soft-tissue density within the vitreous; and (*c*) dependent layering of high-attenuation fluid within the vitreous (45). The triangular intravitreal structure represents persistent tissue along Cloquet's canal and can be seen to enhance densely after contrast administration (37). Associated features may include microphthalmia, retinal detachment, and cataract formation (45). The CT findings of Coats disease include retinal detachment and a high-attenuation subretinal exudate (38). The CT findings of ocular toxocariasis are a focal intraocular mass, which is often associated with thickening of the uveoscleral coat, reflecting longstanding inflammation (38). Contrast enhancement is absent or only mild (37, 38).

Cross-sectional imaging studies are important to evaluate orbital and intracranial invasion. CT imaging should include axial and coronal 3- to 5-mm section imaging of both orbits, to assess intraorbital extension as well as determine whether the tumor is bilateral. On occasion, large necrotic retinoblastomas can produce orbital inflammatory changes on CT that mimic orbital invasion (46). Contrast-enhanced imaging of the brain should be performed in patients with bilateral retinoblastoma, with special attention to the pineal region, because of the risk of an independent primary intracranial tumor (37).

MR

The MR appearance of retinoblastoma is that of a mass that is isointense or slightly hyperintense relative to vitreous on T1-weighted images and hypointense on T2-weighted images (37, 38, 44). As expected, calcifications, which are helpful in establishing the diagnosis on CT, are difficult to detect on MR imaging (37). MR offers, in some cases, advantages over CT, such as distinguishing retinoblastoma from accompanying subretinal fluid (47) and noncalcified lesions from other primary retinal and vitreal abnormalities that simulate retinoblastoma (38). For example, Coats disease and ocular toxocariasis can be difficult to distinguish from noncalcified retinoblastoma on CT (38, 44). However, the subretinal exudate of Coats disease is hyperintense on all MR pulse sequences, whereas retinoblastoma is hypointense on T2-weighted images (37, 38). *Toxocara* granuloma is also hyperintense on all pulse sequences, and the hyperintense appearance on T2-weighted images is, therefore, helpful in distinguishing it from retinoblastoma (44). Persistent hyperplastic primary vitreous can be distinguished from retinoblastoma on MR imaging by the presence of hyperintense fluid-fluid levels on T1-weighted images reflecting hemorrhage within the vitreal chamber as well as hyperintense subretinal fluid caused by retinal detachment (37).

MR also plays an important role in detecting intracranial extension of retinoblastoma. The spectrum of central nervous system metastasis on cross-axial imaging studies includes meningeal or ependymal enhancement, intraventricular and subependymal nodules, intraparenchymal metastases of various sizes (which are sometimes shown to have CT or MR imaging features of hemorrhage), and ventricular dilatation (42, 48).

Ultrasonography

Retinoblastomas usually have an irregular shape on ultrasound examination, with a high internal reflectivity caused by calcification (49). The calcifications may be dense, resulting in shadowing of the adjacent structures. Alternatively, the calcifications may be small and scattered throughout the mass. Limitations of ultrasonography include difficulty in determining extension into the optic nerve, in part because of shadowing cause by calcifications (49).

Treatment

Retinoblastoma

Enucleation is the most common treatment for retinoblastoma. When bilateral tumors are present, the more severely affected eye is generally enucleated. An attempt is made to remove as long a segment of the optic nerve as possible, because the optic nerve is the main route of tumor extension

(50). Recent advances in the development of conservative therapies, including photocoagulation, therapeutic irradiation using external-beam radiotherapy or radioactive eye plaques, and chemotherapy, have led to salvage of the affected eye and maintenance of vision in many cases (50, 51).

Coexistent Retinoblastoma and Pinealoblastoma

Treatment of the pinealoblastoma associated with bilateral retinoblastomas is complicated by the fact that intracranial and spinal dissemination may be present at the time of diagnosis. Craniospinal irradiation in combination with systemic and intrathecal chemotherapy has been advocated for treatment of these highly aggressive tumors (52).

Prognosis

Retinoblastoma

The survival rate for retinoblastoma is generally good in developed countries because of early diagnosis. Survival rates for unilateral retinoblastoma have been reported at 93% at 5 years and 92% at 10 years and for bilateral tumors at 92% at 5 years and 87% at 10 years (53). Successful therapy depends, in large part, on extent of tumor at the time of diagnosis (1). There is a high rate of cure when retinoblastoma is confined to the globe (54), but prognosis is poor when the tumor extends into the optic nerve or the orbit (42, 53). Patients with either unilateral or bilateral retinoblastoma are at risk for the development of second nonocular tumors (most commonly sarcomas) regardless of whether they have received radiation therapy (53, 55).

Coexistent Retinoblastoma and Pinealoblastoma

Coexistent retinoblastoma and pinealoblastoma is associated with a particularly poor course (52), with a high rate of subarachnoid tumor spread (10, 11, 13). In the absence of treatment, mean survival after diagnosis of the intracranial tumor is 1.3 months (12); mean survival after treatment is 9.7 months (13).

References

1. Helveston EM, Knuth KR, Ellis FD. Retinoblastoma. *J Pediatr Ophthalmol Strabismus* 1987;24:296–300
2. Pendergrass TW, Davies S. Incidence of retinoblastoma in the United States. *Arch Ophthalmol* 1980;98:1204–1210
3. Zimmerman RA, Bilaniuk LT. CT in the evaluation of patients with bilateral retinoblastomas. *J Comput Assist Tomogr* 1979; 3:251–257
4. Young JL Jr, Ries LG, Silverberg E, Horm JW, Miller RW. Cancer incidence, survival and mortality for children younger than age 15 years. *Cancer* 1986;58:(suppl 2):598–602
5. Abramson DH. Retinoblastoma: diagnosis and management. *CA Cancer J Clin* 1982;32:130–140
6. Ellsworth RM. Retinoblastoma. In Tasman W, ed. *Duane's Clinical Ophthalmology*. Vol 3. Philadelphia: JB Lippincott, 1989;35:1–19
7. Haik BG, Siedlecki A, Ellsworth RM, Sturgis-Buckout L. Documented delays in the diagnosis of retinoblastoma. *Ann Ophthalmol* 1985;17:731–732
8. Shields CL, Shields JA, Shah P. Retinoblastoma in older children. *Ophthalmology* 1991;98:395–399
9. Jakobiec FA, Tso MO, Zimmerman LE, Danis P. Retinoblastoma and intracranial malignancy. *Cancer* 1977;39: 2048–2058
10. Bader JL, Meadows AT, Zimmerman LE, Rorke LB, Voute PA, Champion LA, Miller RW. Bilateral retinoblastoma with ectopic intracranial retinoblastoma. *Cancer Genet Cytogenet* 1982;5: 203–213
11. Pesin SR, Shields JA. Seven cases of trilateral retinoblastoma. *Am J Ophthalmol* 1989;107:121–126
12. Johnson DL, Chandra R, Fisher WS, Hammock MK, McKeown CA. Trilateral retinoblastoma: ocular and pineal retinoblastomas. *J Neurosurg* 1985;63:367–370
13. Holladay DA, Holladay A, Montebello JF, Redmond KP. Clinical presentation, treatment, and outcome of trilateral retinoblastoma. *Cancer* 1991;67:710–715
14. Bullock JD, Campbell RJ, Waller RR. Calcification in retinoblastoma. *Invest Ophthalmol Vis Sci* 1977;16:252–255
15. Char DH, Hedges TR. Retinoblastoma. *Ophthalmology* 1984; 91:1347–1350
16. Danziger A, Price MI. CT findings in retinoblastoma. *AJR Am J Roentgenol* 1979;133:695–702
17. Arrigg PG, Hedges TR, Char DH. Computed tomography in the diagnosis of retinoblastoma. *Br J Ophthalmol* 1983;67:588–591
18. Karr DJ, Kalina RE. Computerized tomography fails to show calcification in diffuse retinoblastoma. *J Pediatr Ophthalmol Strabismus* 1991;28:14–16
19. Mansour AM, Greenwald MJ, O'Grady R. Diffuse infiltrating retinoblastoma. *J Pediatr Ophthalmol Strabismus* 1989;26: 152–154
20. Russell DS, Rubinstein LJ. *Pathology of Tumours of the Nervous System*. 5th ed. Baltimore: Williams and Wilkins, 1989: 353–365
21. Burger PC, Scheithauer BW, Vogel FS. *Surgical Pathology of the Nervous System and Its Coverings*. 3rd ed. New York: Churchill, Livingston, 1991:387
22. Perentes E, Rubinstein LJ, Herman MM, Donoso LA, Collins VP. S-Antigen immunoreactivity in human pineal glands and pineal parenchymatous tumor: a monoclonal antibody study. *Acta Neuropathol (Berl)* 1986;71:224–227
23. Knudsen AGJ. Mutation and cancer: statistical study of retinoblastoma. *Proc Natl Acad Sci USA* 1971;68:820–823

24. Cavenee WK, Dryja TP, Phillips RA, et al. Expression of recessive alleles by chromosomal mechanisms in retinoblastoma. *Nature* 1983;305:779–784
25. Horowitz JM, Yandell DW, Park SH, et al. Point mutational inactivation of the retinoblastoma antioncogene. *Science* 1989;243:937–940
26. Sopta M, Gallie BL, Gill RM, et al. The retinoblastoma protein and the cell cycle. *Semin Cancer Biol* 1992;3:107–112
27. Gallie BL, Squire JA, Goddard A, et al. Mechanism of oncogenesis in retinoblastoma. *Lab Invest* 1990;62:394–408
28. Squire J, Gallie BL, Phillips RA. A detailed analysis of chromosomal changes in heritable and non-heritable retinoblastoma. *Hum Genet* 1985;70:291–301
29. Gallie BL, Ellsworth RM, Abramson DH, Phillips RA. Retinoma: spontaneous regression of retinoblastoma or benign manifestation of the mutation? *Br J Cancer* 1982;45:513–521
30. Eagle RCJ, Shields JA, Donoso L, Milner RS. Malignant transformation of spontaneously regressed retinoblastoma, retinoma/retinocytoma variant. *Ophthalmology* 1989;96:1389–1395
31. Gallie BL, Dunn JM, Chan HS, Hamel PA, Phillips RA. The genetics of retinoblastoma: relevance to the patient. *Pediatr Clin North Am* 1991;38:299–315
32. Roarty JD, McLean IW, Zimmerman LE. Incidence of second neoplasms in patients with bilateral retinoblastoma. *Ophthalmology* 1988;95:1583–1587
33. Lindahl S. Computed tomography of retinoblastoma. *Acta Radiol Diagn* 1986;27:513–518
34. Shields JA, Parsons HM, Shields CL, Shah P. Lesions simulating retinoblastoma. *J Pediatr Ophthalmol Strabismus* 1991;28:338–340
35. Sebag J. Vitreous pathobiology. In: Tasman W, ed. *Duane's Clinical Ophthalmology*. Vol 3. Philadelphia: JB Lippincott, 1989;39:1–26
36. Duker JS, Brown GC. Vascular anomalies of the fundus. In: Tasman W, ed. *Duane's Clinical Ophthalmology*. Vol 3. Philadelphia: JB Lippincott, 1989;22:1–12
37. Weber AL, Mafee MF. Evaluation of the globe using computed tomography and magnetic resonance imaging. *Isr J Med Sci* 1992;28:145–152
38. Mafee MF, Goldberg MF, Greenwald MJ, Schulman J, Malmed A, Flanders AE. Retinoblastoma and simulating lesions: role of CT and MR imaging. *Radiol Clin North Am* 1987;25:667–682
39. Margo CE, Katz NNK, Wertz FD, et al. Sclerosing endophthalmitis in children: computed tomography with histopathologic correlation. *J Pediatr Ophthalmol Strabismus* 1983;20:180–184
40. Jakobiec FA, Rootman J, Jones IS. Secondary and metastatic tumors of the orbit. In: Tasman W, ed. *Duane's Clinical Ophthalmology*. Vol 2. Philadelphia: JB Lippincott, 1989;46:1–67
41. MacKay CJ, Abrahamson DH, Ellsworth RM. Metastatic patterns of retinoblastoma. *Arch Ophthalmol* 1984;102:391–396
42. Meli FJ, Bocclaeri CA, Manzitti J, Lylyk P. Meningeal dissemination of retinoblastoma: CT findings in eight patients. *AJNR Am J Neuroradiol* 1990;11:983–986
43. Picard L, Almeras M, Delgoffe C, et al. Medulloblastomas and retinoblastomas: CT images of intracranial meningeal metastases. *J Neuroradiol* 1983;10:43–49
44. Mafee MF, Goldberg MF, Cohen SB, et al. Magnetic resonance imaging versus computed tomography of leukocoric eyes and use of in vitro proton magnetic resonance spectroscopy of retinoblastoma. *Ophthalmology* 1989;96:965–976
45. Mafee MF, Goldberg MF. Persistent hyperplastic primary vitreous (PHPV): role of computed tomography and magnetic resonance. *Radiol Clin North Am* 1987;25:683–692
46. Shields JA, Shields CL, Suvarnami C, et al. Retinoblastoma manifesting as orbital cellulitis. *Am J Ophthalmol* 1991;112:442–449
47. Sullivan JA, Harms SE. Characterization of orbital lesions by surface coil MR imaging. *Radiographics* 1987;7:9–28
48. Atlas SW, Kemp SS, Rorke L, Grossman RI. Hemorrhagic intracranial retinoblastoma metastases: MR-pathology correlation. *J Comput Assist Tomogr* 1988;12:286–289
49. Byrne SF, Green RL. *Ultrasound of the Eye and Orbit.* St Louis: Mosby-Year Book, 1992;5:133–213
50. Shields JA. Misconceptions and techniques in the management of retinoblastoma. *Retina* 1992;12:320–330
51. Zelter M, Damel A, Gonzalez G, Schwartz L. A prospective study on the treatment of retinoblastoma in 72 patients. *Cancer* 1991;68:1685–1690
52. Nelson SC, Friedman HS, Oakes WJ, et al. Successful therapy for trilateral retinoblastoma. *Am J Ophthalmol* 1992;114:23–29
53. Committee for the National Registry of Retinoblastoma. Survival rate and risk factors for patients with retinoblastoma in Japan. *Jpn J Ophthalmol* 1992;36:121–131
54. Redler LD, Ellsworth RM. Prognostic importance of choroidal invasion in retinoblastoma. *Arch Ophthalmol* 1973;90:294–296
55. Abramson DH, Ellsworth RM, Kitchin FD, Tung G. Second nonocular tumors in retinoblastoma survivors: are they radiation-induced? *Ophthalmology* 1984;91:1351–1355

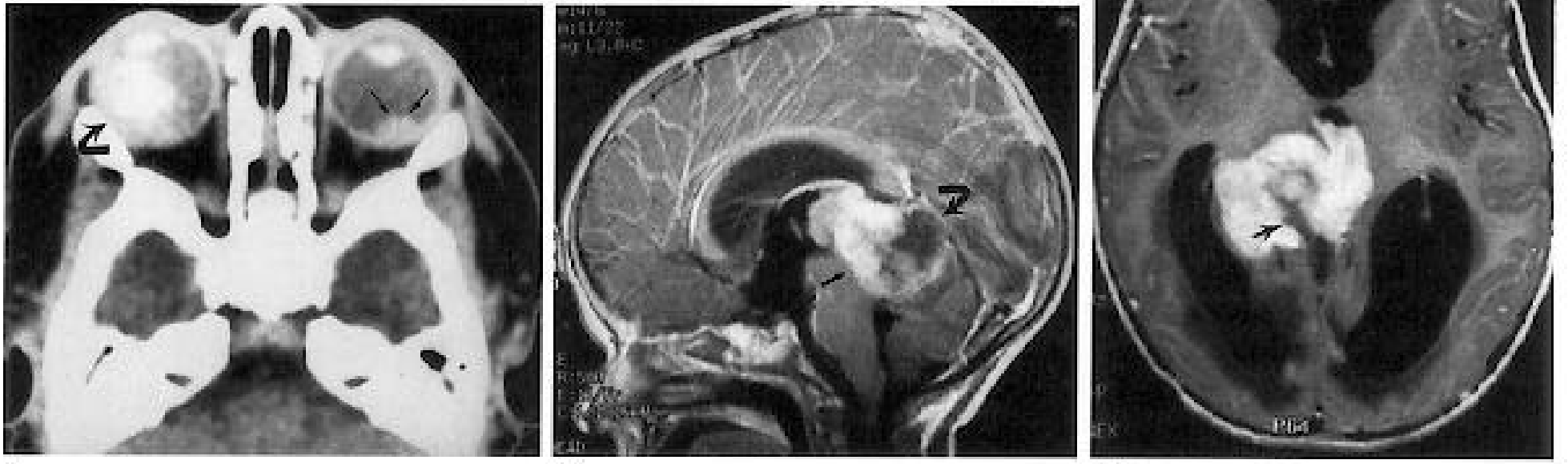
A
B
C

D

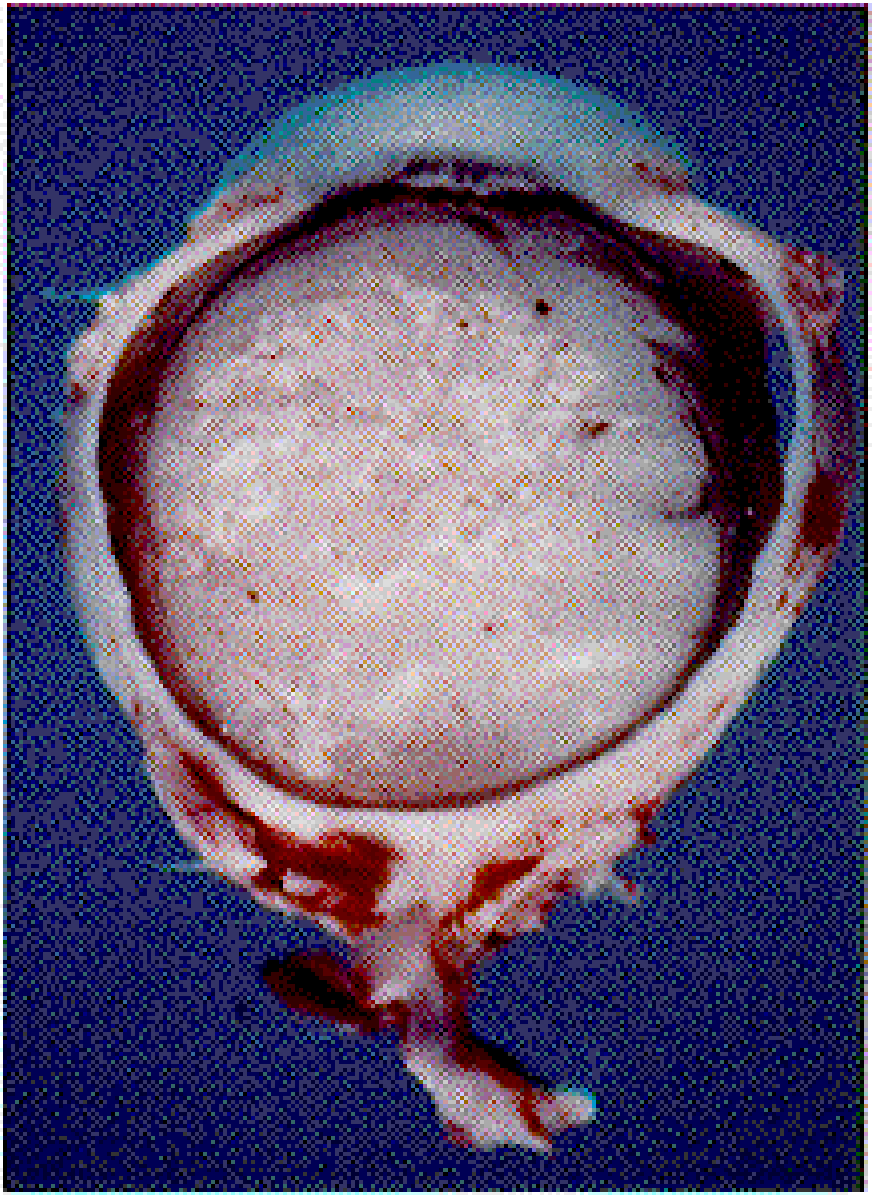

E

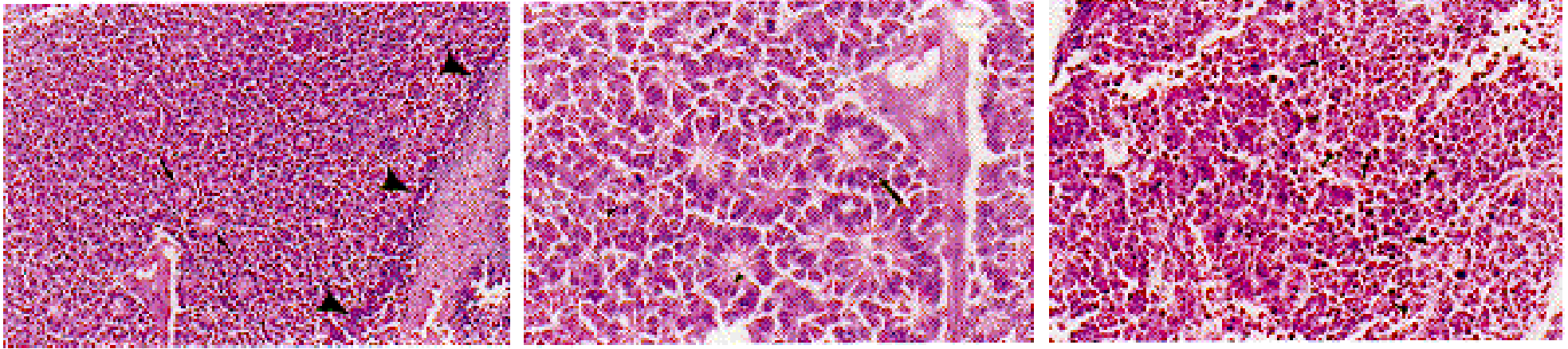

F G H